Research Article

Anti-Proliferative and Apoptotic Effects of Aflatoxin B1 Purified from *Aspergillus Flavus* of Stored Wheat Grains in India on Human Cells - ♾

Ranjana Kumari[1], Harsh Jaiswal[1], Rashmi Bharti[2], Lakshmi E Jayachandran[3], Ananta K Ghosh[1]*

[1]*Department of Biotechnology, Indian Institute of Technology Kharagpur, India*
[2]*School of Medical Science & Technology, Indian Institute of Technology Kharagpur, India*
[3]*Department of Agriculture and Food Engineering, Indian Institute of Technology Kharagpur, India*

*Address for Correspondence: Ananta K. Ghosh, Department of Biotechnology, Indian Institute of Technology Kharagpur, Kharagpur, West Bengal 721302, India, E-mail: aghosh@bt.iitkgp.ac.in

ABSTRACT

Aflatoxins are commonly produced by *Aspergillus flavus* present in stored food grains. Among different aflatoxins, the chemo type AFB_1 is highly carcinogenic and produces a cascade of events in many organs of the affected organisms to exert its toxic effects. Aflatoxin was extracted from the culture media of *Aspergillus flavus* isolated from stored wheat grains in India and then AFB_1 was purified to homogeneity by a series of chromatographic procedures. The anti-proliferative and apoptotic effect of AFB_1 on human hepatoma (HepG2) and embryonic kidney cells (HEK293) were studied *in vitro* by MTT assay and IC_{50} was determined as 12.8 μM and 19.2 μM, respectively. The toxin treatment caused nuclear fragmentation, chromatin condensation and induced apoptosis through the up regulation of the stress and apoptotic genes like Bax, caspase-3, and cytochrome C, along with the down regulation of anti-apoptotic Bcl-2 gene. Cell cycle analyses showed that AFB_1 arrests cell growth in sub G1 phase, binds to DNA and these effects depend on its concentration, time of exposures, and cell type. These results suggest the importance of proper detoxification and control measures of AFB_1 contamination in food and feed to protect human and animal health.

Keywords: Aflatoxin B_1; Purification; Human Cell Line; Cytotoxicity; Apoptosis

INTRODUCTION

Fungal infestation is a leading cause of stored grain losses across the world. Fungi of stored food grains have been associated with production of mycotoxins, which poses a serious health hazard to human and animal population. Toxigenic fungi have been isolated from various food grains stored in warehouses across the different agroclimatic zones of the country. Among all the mycotoxins detected in stored grains, aflatoxin is the most common form, mainly produced by *Aspergillus flavus*. Out of four aflatoxin chemotypes (B_1, B_2, G_1 and G_2), AFB_1 is most toxigenic [1] and classified as a class 1 human carcinogen by the International Agency for Research on Cancer. More than 55 billion people worldwide suffer from uncontrolled exposure to aflatoxins, which accounts for 4.6–28.2% of all global hepatocellular carcinoma [2]. Exposure of aflatoxins to an organism produces a cascade of events in more than one organ. Aflatoxins have different adverse health effects like hepatotoxicity, genotoxicity and immunotoxicity in humans and several other animal species. The liver and kidney are the main organs responsible for metabolism and detoxification, and thus primarily affected by aflatoxin ingestion [3]. The aflatoxin is metabolized by cytochrome P-450 enzymes to reactive exo-8,9-epoxide to induce the formation of DNA adducts which leads to mutation of tumour suppressor gene p53 and subsequently development of hepatocellular carcinoma [4, 5].

Several studies have been performed to analyse the individual and combined effect of aflatoxin chemotypes on different cell lines [6,7,8,9,10] and it has been shown that the effect of aflatoxin varies with its chemotypes, dose, length of exposure as well as affected animal species, its age and nutritional status [9,11] suggesting that elaborate studies are needed to decipher cell or animal-specific mechanism of action of different aflatoxin types.

We have reported earlier *Aspergillus flavus* as the predominant fungus in stored wheat grains in different warehouses of the Food Corporation of India within the state of West Bengal [12]. The aflatoxin production by the isolated strains is confirmed by ammonia vapour test, Thin Layer Chromatography (TLC) and High-Performance Liquid Chromatography (HPLC). The current study has been undertaken for the extraction and purification of aflatoxin chemotype AFB_1 from toxigenic *A. flavus* strain isolated from the stored wheat grains in India, and analysis of its carcinogenic effect on immortalized human liver (HepG2) and kidney (HEK293) cell lines. The study of aflatoxin toxicity and mechanism of action on different human cell lines could help in the development of measures to reduce its toxic effects on to human and animal health.

MATERIALS AND METHODS

Purification of aflatoxins

Aflatoxigenic *A. flavus* (previously isolated in our lab from stored what grains) were cultured on Yeast Extract Sucrose (YES) media (2% yeast extract, 20% sucrose and 20% sucrose) in broth as well as on culture plate for 14 days at 30⁰C. The broth of fungal culture (100 ml) was mixed with an equal volume of chloroform for 12 h with shaking to extract toxin in the solvent phase. Fungi grown on solid media (20 g) were crushed in 100 ml of acetonitrile: methanol (85:15) mixture and filtered through Whatman paper to remove debris and fungal spores. The organic solvent extracted toxins from both the solid and liquid media were centrifuged at 10000xg for 10 min and the supernatants were concentrated in a rotary evaporator (Model: Rotavapor R- 210; Make: Büchi Labortechnik AG, Flawil, Switzerland) to the final volume of 1 ml. The presence of different aflatoxins in the extract were checked by Thin Layer Chromatography (TLC) on pre-coated silica gel 60 aluminium plate (20 × 20 cm) using toluene: ethyl acetate: formic acid (6:3:1) as mobile phase solvent and visualized under UV light at 365 nm.

Purification of AFB_1 by Silica gel column chromatography, semi preparative and analytical HPLC

A glass column (22 mm x 300 mm) packed with silica beads was prepared as follows: Initially an empty column was filled with chloroform and to it 5 g sodium sulphate was added to prepare a bottom layer. Then, 10 g of silica beads (pre swelled in chloroform) and 5 g sodium sulphate were added to prepare the upper layer. The column was washed with 150 ml of chloroform at the flow rate of 0.5 ml/min to remove all the bubbles. In this packed column 1 ml of concentrated aflatoxin extract was loaded and after the aflatoxins enter into the column bed completely, it was washed initially with 10 ml of hexane and then with 10 ml of diethyl ether to remove lipids and fats. Thereafter, aflatoxins were eluted in 10 ml of varying concentration of chloroform: methanol (97:3; 99:1) mixture and with 100% methanol. All elutes were concentrated in rotary evaporator, analysed by TLC and visualized under UV light.

The concentrated toxin from silica gel column was dissolved in acetonitrile (100%) and separated through semi-preparative High Performance Liquid Chromatography (HPLC) (Model: 1260 Series; Make: Agilent, USA) using SBC18 column (9.4 mm x 250 mm) and acetonitrile: water (80:20) as mobile phase solvent in isocratic mode for 50 min at the flow rate of 1ml/min. Elution was monitored in diode array detector, peak fractions were collected separately, concentrated and analysed by TLC.

The major elutes (containing aflatoxins) from the semi-preparative HPLC column was further purified through reverse-phase analytical HPLC (Model: 1260 Series; Make: Agilent, USA) fitted with SBC18 column (5 μm, 4.6 mm x 250 mm), in an isocratic mode using H_2O: methanol: acetonitrile (6:3:1) as mobile phase solvent at flow rate 1 ml/min. All the peak fractions (containing different aflatoxin chemo-types) were eluted separately and the purity of eluted toxin in each peak was again checked by TLC and analytical HPLC by monitoring in Diode array detector (DAD; λ = 365/20 nm) and fluorescence detector (FLD; λ = 365 nm excitation, λ= 450 nm emission). The concentration of purified AFB_1 chemotype was determined by measuring OD at 360 nm and comparing with standard curve of pure AFB_1 (Sigma).

Molecular weight determination of AFB1 by MALDI-TOF mass spectrometer

The molecular weight of purified AFB_1 was determined in a MALDI-TOF mass spectrometer (Model: Ultraflex III TOF/TOF; Make: Bruker Daltonics). The purified AFB_1 was mixed with α-cyano-4-hydroxycinnamic acid (HCCA) matrix (1:1), and 1.0 μl of this mixture was spotted on target plate. The plate was allowed to dry in air and then the spectra were recorded in the positive ion linear mode.

Anti-proliferative activity assay of AFB1 on human cell lines *in vitro*

Anti-proliferative effects of AFB1 on HEK293 and HepG2 cells were evaluated by MTT assay [13]. In brief, human liver (HepG2) and kidney (HEK293) cells were cultured in RPMI-1640 and DMEM media, respectively supplemented with 10% fetal bovine serum, 100 units per ml of penicillin, and 100μg/ml streptomycin in a humidified incubator containing 5% CO_2 and 95% air at 37°C by sub- culturing every 3-4 days interval. Cell number was determined by counting in a haemocytometer. 5 x 10^3 cells in 200 μL of media were seeded into individual wells of 96-well micro plates (Tarsons, India). Cells were allowed to grow for 24 hrs and the culture medium was replaced by fresh medium containing different concentrations of purified AFB_1 (0.8, 1.6, 3.2, 6.4, 12.8, 19.2, 25.6, and 51.2 μM). The cells were incubated for another 48 hrs, spent media was replaced with fresh serum free media containing 100 μl of MTT [3-(4, 5-dimethylthiazol-2-yl)-2,5-diphenyl tetrazolium bromide] solution (5 mg/ml) and incubated for another 4 hrs at 37°C in a CO_2 incubator for the formation of formazan crystal in the well. The crystals were dissolved by adding 100 μl of DMSO in each well and the OD was measured at 570 nm. Experiments for both the cell lines using different concentration of AFB_1 were done in triplicates. The percentage of living cells was calculated using following formula:

$$Percentage\ of\ living\ cell = \frac{(OD\ of\ treated\ well\ -\ OD\ of\ blank\ well)}{(mean\ OD\ of\ untreated\ well\ -\ OD\ of\ blank\ well)} x100$$

Dose-dependent viability response curve was prepared and the concentration of toxin which causes 50% of cell death was taken as inhibitory concentration 50 (IC_{50}).

Live/Dead cell staining and chromatin condensation assay

To visualize the live or dead cells (HepG2 an HEK293) after treatment with AFB_1, cells were stained acridine orange (AO) and ethidium homodimer-1 (EB) as per the manufacturer's (Sigma) protocol. In brief, within the wells of cell culture plate (12 wells) circular coverslips (18 mm) were placed and soaked in 70% ethanol

for overnight. Thereafter, cover slips were rinsed three times with 1 x PBS (pH 7.4) and again submerged in complete media for 2 hrs for conditioning. In each well 200 μl of cells (5x10^3) were added and incubated for 24 hrs in CO_2 incubator at 37°C. Then spent media was replaced with fresh media containing AFB_1 at its IC_{50} concentration (12.8 μM in case of HepG2 cells and 19.2 μM in case of HEK293 cells) and incubated for another 48 hrs. Thereafter, cells were dislodged from the plate using trypsin, washed with 1x PBS and 10 μl of cell suspension was taken on a glass slide. Then 1 μl of acridine orange (AO) and ethidium homodimer-1 (EB) solution (1:1 v/v) [final concentration of 100 μg/ml], was added to it and covered with a coverslip. The stained cells were then observed in a fluorescent microscope (Make: Nikon Instruments Inc., USA, Model: Eclipse TS100-F) and photographed.

For checking the chromatin condensation, cells grown on coverslips were fixed by treating with 3.7% paraformaldehyde for 30 min at room temperature, washed with 1 x PBS and permeabilized with treatment of 0.1% Triton-X-100. The permeabilized cells were again washed with 1x PBS, stained with 10 μl of DAPI (4, 6-diamidino-2-phenylindole) solution (100 μg/ml) (Thermo fisher scientific, USA) and covered with cover slip. Stained cells were observed under a confocal laser scanning microscope (Olympus FluoView FV1000, Version 1.7.1.0, Tokyo, Japan). Images were captured and analysed using FluoView 1000 (version 1.2.4.0) software.

Cell analysis by flow cytometer

The apoptotic effect of AFB1 on HEK293 and HepG2 cells was also analysed by flow cytometer (Model: FACS Calibur; Make: Becton Dickinson, USA,) after staining with propidium iodide (PI) and annexin V-FITC (Sigma, St. Louis, MO). In brief, HEK293 and HepG2 cells (1x 10^6) were seeded separately in 60 mm petri plate, grown for 24 hrs and then treated with IC_{50} dose of AFB_1 (12.8 μM in case of HepG2 cells and 19.2 μM in case of HEK293 cells) for another 48 hrs. The cells were then detached from the petri plate by treating with trypsin-EDTA, washed twice with cold PBS and centrifuged at 1000 rpm for 5 min. The cell pellets were fixed in 70% ice cold ethanol, washed, resuspended in 200 μl PBS and stained by adding 10 μl propidium iodide solution (10 μg/ml). The cells were then analysed in a flow cytometer to calculate changes in sub G1 cell population by analysing different phases of cell cycle.

The cell population undergoing in different stage of apoptosis (after treatment with AFB_1) was analysed in flow cytometer after staining cells with dual marker annexin V-FITC and propidium iodide (PI). Both the cell types were treated with AFB_1 as mentioned above, collected by centrifugation and washed with PBS. The harvested cells were suspended in 400 μl of 1x binding buffer (10 mM HEPES, pH 7.4, 14 mM NaCl and 0.25 mM $CaCl_2$), To these cells 10 μl of each annexin V-FITC (100 μg/ml) and PI (1 mg/ml) were added and incubated at 37°C for 5 min. The stained and unstained cells were immediately analysed in a flow cytometer (FACS Calibur; Make: Becton Dickinson).

Gene expression analysis by western blot

To analyse alteration of gene expression in AFB_1 treated cells, the apoptotic signalling pathway marker genes such as Bax, Bcl-2, p53, and Caspase-3 were analysed by western blot assay. The AFB_1 treated and untreated (control) cells were lysed in 1 ml of lysis buffer (150 mM NaCl, 50 mM Tris (pH 8.0), 5 mM EDTA, 1% (vol/vol) Nonidet p-40, 1 mM phenyl methyl sulfonyl fluoride (PMSF), 20 μg/ml aprotinin,

and 25 µg/ml leupeptin for 30 minutes at 4 ^{0}C, centrifuged at 10,000 x g for 10 min and clear supernatants were collected. The amount of protein present in the supernatant was estimated by the method of Bradford using BSA as standard [14]. Equal amounts (50 µg) of each protein extracts were resolved by 10% SDS-polyacrylamide gel electrophoresis (SDS-PAGE) and electro transferred to nitrocellulose membrane. After transfer, the membranes were incubated in blocking buffer [20 mM Tris-HCl (pH 7.5), 500 mM NaCl, and 5% non-fat milk] for 2 hrs at room temperature and then incubated over night with mouse antibodies (diluted in PBS) specific for Bcl-2 (1/500, v/v), Bax (1/250, v/v), cytochrome C (1/200, v/v), β-actin (1/1000,v/v) and cleaved caspase 3 (1/500, v/v) (Calbiochem, Cambridge, MA). The membranes were then washed with PBST (PBS containing 0.1% Tween 20) and incubated with secondary antibody (anti-mouse IgG) conjugated with horseradish peroxidase (HRP) (1/5000, v/v) for 1 hr. The blots were again washed with PBST, developed using a chemiluminescent reagent (ECL; Amersham Life Science, Buckinghamshire, UK) and photographed.

**Analysis of AFB1 binding with genomic DNA**

To analyse the interaction of aflatoxin with genomic DNA of animal cells, DNA binding assay was performed. Genomic DNA from HepG2 cells was extracted by standard procedure [15] and two different sets of experiments were performed. In the first set fixed concentration of AFB$_1$ (25.6 µM) was mixed with varying concentration of HepG2 genomic DNA (1, 2, 3, 4, and 5 µg) in1 ml of PBS and in second set, fixed concentration of genomic DNA (2 µg) was mixed with varying concentration of AFB$_1$ (6.4, 12.8, 19.2, 25.6, and 51.2 µM). The AFB$_1$-DNA mixtures were incubated for 1 hr at room temperature and then changes in absorption spectra were recorded in a spectrophotometer at 200–500 nm wavelength of light [16].

RESULTS AND DISCUSSION

Extraction and purification of aflatoxin B$_1$

AFB$_1$ chemotype was extracted from the broth and solid media culture of *A. flavus* by organic solvent extraction (chloroform and methanol or acetonitrile and methanol) followed by silica gel chromatography. TLC plate analysis showed the production of four different chemo-types of AFB$_1$, AFB$_2$, AFG$_1$ and AFG$_2$ along with several other pigments after silica gel column chromatography [Figure 1(d), lane 4]. The aflatoxins extracted from the YES agar plate showed more amount of aflatoxin production than the YES broth. Further purification was done by semi-preparative HPLC. Elution profile from the semi-preparative HPLC showed presence of one major peak and several minor peaks [Figure 1(a)]. Analyses of the contents of major peak by TLC also showed presence of two major aflatoxins and several minor components [Figure 1(d), lane 3]. Re-analyses of this major peak fraction by analytical HPLC showed one major peak of AFB$_1$ and one minor peak of AFB$_2$ (in respect to similar analysis of standard aflatoxin chemo types) [(Figure 1(b)]. Further analysis of this analytical HPLC purified AFB1 by another analytical HPLC showed a single peak [(Figure 1(c)] and a showed single spot in TLC [Figure 1(d), lane 2] migrating in the similar position of standard AFB$_1$ indicating purification of AFB$_1$ to homogeneity. MALDI-TOF mass spectrometry revealed the molecular weight of purified AFB$_1$ as 313.663 Da [Figure 1(e)]. The concentration of purified AFB1 was determined by measuring OD at 360 nm and using the standard curve AFB$_1$ from Sigma (Figure S1)
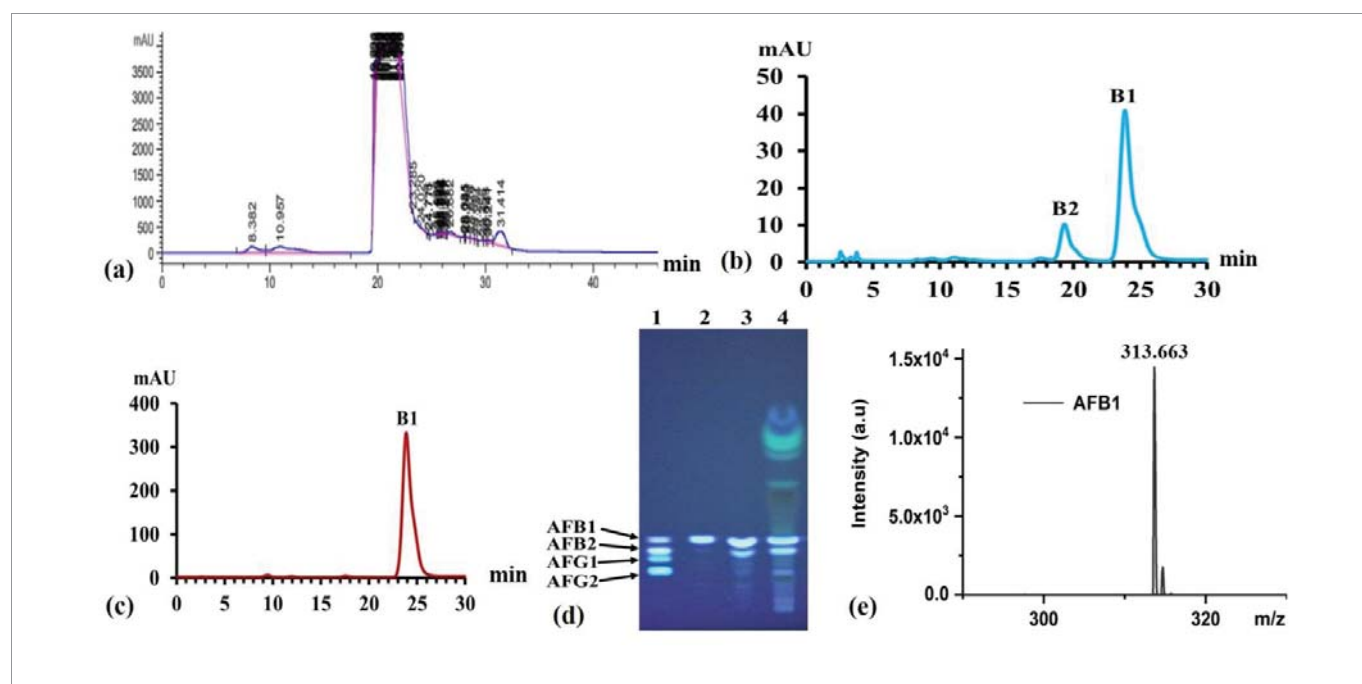
Figure 1: Extraction and purification of AFB$_1$ by various chromatographic techniques: a) Elution profile of extracted aflatoxin (from silica gel column) in semi-preparative HPLC, b) Elution profile of major peak fraction (from semi-preparative HPLC) in analytical HPLC, c) Elution profile of AFB$_1$ in analytical HPLC, d) Separation of aflatoxins by TLC ; lane 1, standard aflatoxin mix (Sigma); lane 2, AFB$_1$ purified by analytical HPLC; lane 3, aflatoxins purified by semi-preparative HPLC; lane 4, aflatoxins purified by silica gel column, and e) MALDI-TOF analysis of purified AFB$_1$.
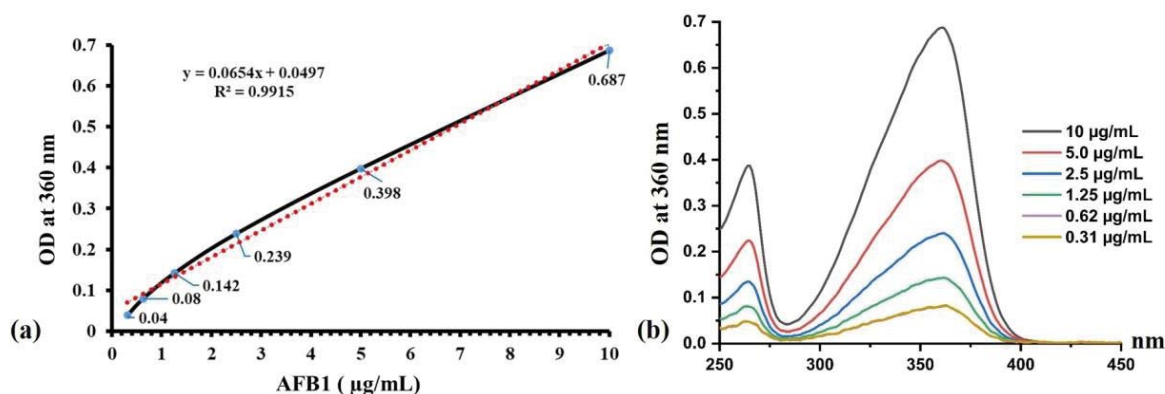
Figure 1: Standard graph for concentration determination of AFB₁ prepared by taking OD at 360 nm of different concentration of AFB₁ dissolved in methanol. (a) Concentration vs OD at 360 nm plot and (b)Uv- visible absorption spectra showing variation of peak intensity with concentration at 360 nm.

Anti-proliferative effect of AFB₁ on HepG2 and HEK293 cells

MTT assay was carried out to evaluate the anti-proliferative potential of AFB₁ on HepG2 and HEK293 cells at the concentration of 0.8, 1.6, 3.2, 6.4, 12.8, 19.2, 25.6, and 51.2 μM. The results showed a decrease in cell viability with the increase in time of exposure and concentration of AFB₁ with some variation between the two cell lines. At low concentration of AFB₁ ($\leq$ 1.6 μM), cell proliferation was observed in both cell lines. A 50% reduction in cell viability (IC50) was observed after 48 hrs at an AFB₁ concentration of 12.8 μM in case of HepG2 cells, and at 19.2 μM AFB₁ concentration in case of HEK293 cells (Figure 2). Observation of these cells under the microscope showed disruption of normal cellular morphology and loss of their intercellular connectivity with the increase of exposure time (Figure 3a).

Previously different IC_{50} values of AFB₁ for different cell lines have been reported. McKean et al [6] have reported IC50 value as 1 μM and 100 μM for human HepG2 cells and BEAS-2B cells (human bronchial epithelial cell line), respectively. Lei et al [17] have observed 38.8 μM as the IC_{50} concentration of AFB₁ in porcine kidney (PK-15) cell line. Similarly, IC_{50} of AFB₁ in Vero cell has been reported as 30 μM after 24 hrs of exposure by MTT assay [18]. These differences in IC_{50} value for different cell lines suggest that AFB₁ exerts its anti-proliferative effect differently on different cell lines. The observed small enhancement of cell proliferation at lower concentration of AFB₁ (<1μM) may be due to alternation in cell physiology that causes an increase in cellular adaptability whereas high concentration damages the cell beyond its limit of recovery leading to death [19].

Observation of cell and nuclear morphology using DAPI and AO/EB stain

Different toxins induce cell death in different pathways such as necrosis and/or apoptosis, and can be distinguished by distinct cellular, morphological and biochemical features [20]. Apoptotic cell death is characterized by nuclear shrinkage and cellular blebbing, without any effect on the membrane integrity. It is also accompanied by chromatin condensation, nuclear fragmentation, and activation of cysteine proteases called caspases. On the other hand, necrotic
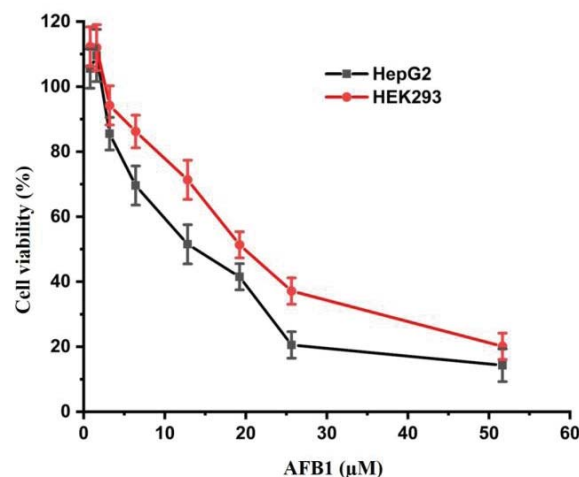
Figure 2: Percentage cell viability relative to control cell upon treatment with AFB₁. Each point represents value as mean ± standard deviation of triplicate experiments.

death pattern is highlighted by swelling and rupture of the nuclear membrane due to increase in cell permeability and membrane integrity, loss of ion gradients, irreversible chromatin condensation, and the release of intracellular contents [21]. In the current study, we have tried to decipher the mechanism of AFB1 induced cell death in human liver and kidney cells by observing changes in cell and nuclear morphology, chromatin condensation using fluorescent dyes, and analysing apoptosis related proteins expression profile.

DAPI is a fluorescent dye that is impermeable to living cells at low concentration. This dye binds strongly with Adenine-Thymine (AT) bases of double stranded DNA and gives 20-fold intense blue fluorescence. It can be employed to investigate the extent of nuclear changes during apoptosis and determine the fraction of apoptotic cells with condensed and fragmented DNA. Observation of DAPI stained untreated HepG2 and HEK293 cells under confocal laser scanning microscope showed uniform diffuse blue fluorescence but the AFB1 treated (24 h onwards) cells showed bright nuclear fluorescence

confirming condensation of chromosome. After 48 h of treatment, the fluorescent dye was observed to be dispersed throughout the cell, indicating extensive nuclear fragmentation (Figure 3b). The chromosome condensation and fragmentation confirmed that cells were dying by apoptotic pathway. The DAPI stain has been used to study the induction of apoptosis by ochratoxins in mammalian cell lines and rat kidney cells [22].

Acridine Orange (AO) dye is permeable to viable cell membrane (vital dye) and stains the cells uniformly with a green color. On the other hand, the Ethidium Bromide (EB) dye can penetrate the dead cells that have lost their membrane integrity. The EB is a DNA intercalating dye that binds with chromosome and gives red fluorescence [23]. Hence, these dyes were used to investigate the nature of cell death (apoptosis and/ necrosis) caused by AFB_1. The examination of control cells (untreated) and AFB_1 treated cells after staining with AO/EB under fluorescent microscope showed uniform green color in control cells even after 48 h of culture whereas treated cells displayed increase in the intensity of red color with respect to treatment time (Figure 3c). The gradual change in fluorescence color from green (live cells) to dark red (late apoptosis cells), through an intermediate yellow fluorescence (early apoptotic cells) confirmed that AFB_1 significantly induced apoptosis in HepG2 and HEK293 cells. This result corroborated the findings of Xu et al [24] on the HepG2 cell line using ligustrazine-triterpenes derivatives.
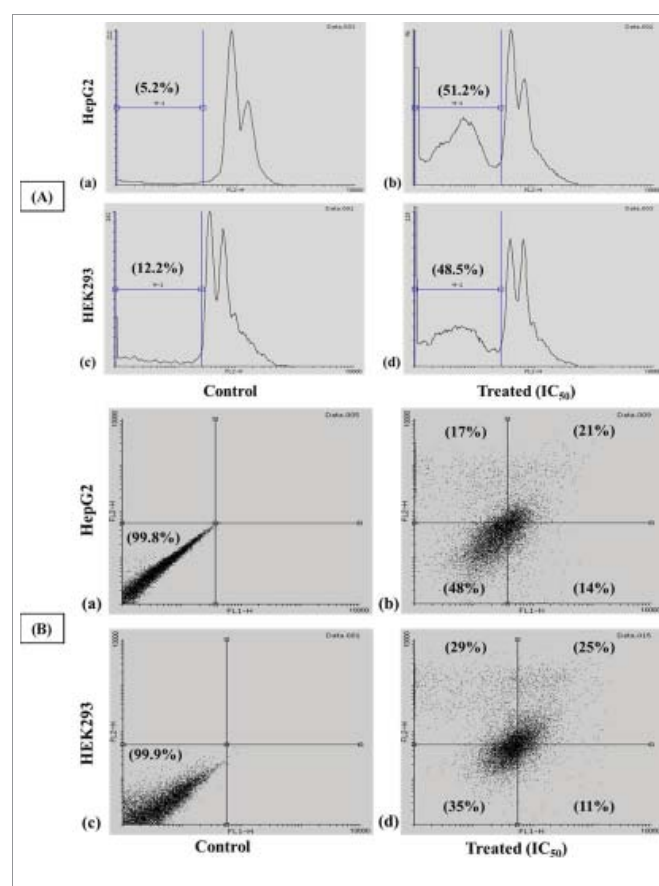
Flow cytometry analysis

To observe the apoptotic effect of AFB_1 on HepG2 and HEK293
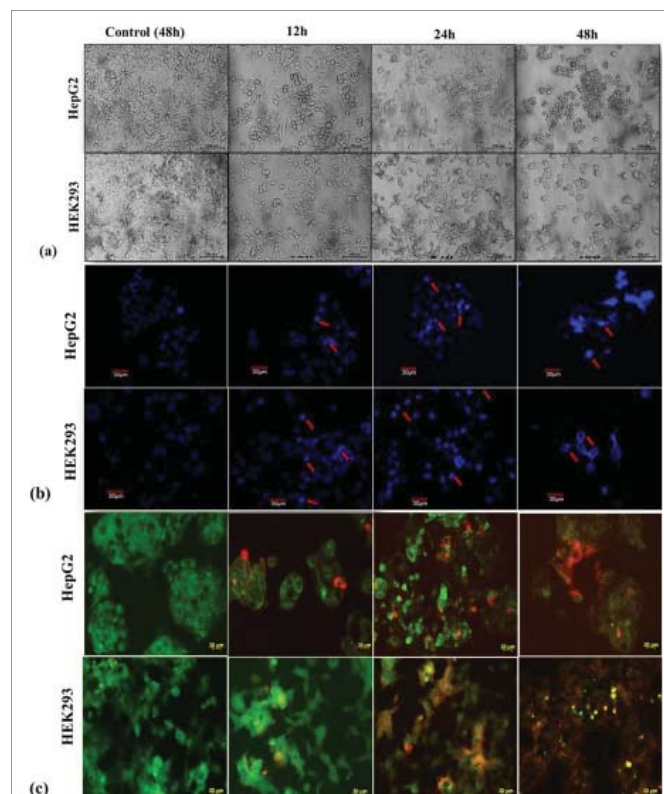
Figure 3: Morphology of AFB_1 treated cells with IC_{50} concentration (12.8 μM in case of HepG2 cells and 19.2 μM in case of HEK293 cells) as observed under (a) phase contrast microscope (b) confocal microscope after staining with DAPI and (c) fluorescence microscope after staining with AO/EB. (Magnification 400 x)

cells, further analysis was performed using annexinV and propidium iodide stain. The live cell expresses phosphatidylserine in cytosolic side of plasma membrane. The cell undergoing apoptosis translocate this compound to extracellular side and make accessible for binding with calcium dependent phospholipid binding proteins like annexin [25]. In flow cytometry, cell cycle analysis of control cells stained with PI showed only 5.2% cell population in sub G1 phase in case of HepG2 while in case of HEK293, it was around 10% of total cell population. For the AFB_1 treated cells, the sub G1 cell population reached around 50% of total cell population in both HepG2 and HEK293 cells (Figure 4A). This sub G1 cell population represents the cells undergoing apoptotic or necrotic cell death. Similar results were observed when the treated cells were studied using both these two-fluorescent dye (annexin V and PI) together. More than 50% of total AFB_1 treated (IC_{50}) cell population were observed in early apoptotic phase (Annexin V+/PI−), late apoptotic phase (Annexin V+/PI+) and necrotic or dead phase (Annexin V−/PI+) and confirmed the apoptotic pathway induced cell death (Figure 4B).

Figure 4: Flow cytometric analysis of AFB_1 treated (48 hrs) cellular apoptosis at IC_{50} concentration (12.8 μM in case of HepG2 cells and 19.2 μM in case of HEK293 cells). Panel (A) shows distribution of cell population in different phases of cell cycle after staining with only propidium iodide and Panel (B) shows changes in the rate of cells undergoing apoptosis after staining with both annexin V and PI.

Analysis of cells by flow cytometry also showed an increase in the percentage of apoptotic cell count with the increase concentration of AFB_1 and confirms the apoptosis event. Similar type of induction of apoptosis by AFB_1 has been reported by feeding the animals with AFB_1 and analysing the effect in the cells/tissues of different organs

like thymus, spleen, intestine, kidney, liver and bursa of fabricius [9,26-31].

Western blot analysis of AFB1 induced apoptotic genes expression

The expression profile of key regulatory proteins of pro-apoptotic pathway such as Bax, caspase-3 and Bcl-2 was monitored in AFB_1 treated and untreated cells by western blot analysis. The results showed increase in the expression of Bax (20 kDa), cleaved caspase-3 (17 and 19 kDa) and cytochrome C (14 kDa) proteins whereas, decrease in the expression of Bcl-2 protein (26 kDa) (Figure 5). The expression of β-actin (45 kDa) was monitored as internal control and did not show any alteration in expression between AFB_1 treated and untreated cells. The upregulation of the expression of apoptosis inducing proteins such as Bax, capsase3 and cytochrome C and downregulation of anti-apoptotic protein (Bcl-2) confirm apoptosis induced cell death due to AFB_1 treatment. More death was observed for HEpG2 cells than HEK293 cell and suggested that the cytotoxicity of AFB_1 on cell cycle progression depends on the concentration of AFB_1, exposure time, as well as cell types. Similar types of up regulation of Bax, capsase 3 and cytochrome C, and down regulation of Bcl-2 in the aflatoxin treated different cells have been reported earlier [18,32]. Creation of oxidative stress on cell lines due to toxin treatment and production of reactive oxygen species (ROS) have been reported in several studies [33-35]. The ROS production disturbs mitochondrial integrity that leads to the expression of apoptosis associated proteins and ultimately directs apoptotic induced cell death [36]

AFB1-DNA adduct formation

The interaction of AFB_1 and DNA was studied by UV-Vis absorption spectroscopy. The DNA molecules contain aromatic bases and phosphate chromophores, which show characteristic intense absorption peak at approximately 260 nm. The AFB_1 molecules also have a characteristic absorption peak at 365 nm. The interaction of a fixed amount of AFB1 with increasing concentration of DNA exhibited hyperchromism with blue shift at 267 nm while AFB_1 peak at 365 nm displayed slight hyperchromism. The interaction between fixed amounts of DNA with increasing concentration of AFB1 showed hyperchromism with gradual red shift from 260 nm (Figure 6). The hyperchromicity may be attributed to external contact (electrostatic binding) or the disruption of the DNA's secondary structure [37]. Binding of aflatoxin with calf thymus DNA in a similar way in its major / minor grooves, and changes in DNA conformation has been reported by (Ma et al [16].

CONCLUSION

The current study has described the extraction and purification of AFB_1 from the culture of *A. flavus* isolated from stored wheat grain in India using silica gel column, semi-preparative and analytical HPLC. The treatment of human liver and kidney cells with this purified AFB_1 leads to chromosome condensation, DNA fragmentation and increases the expression of key regulatory proteins of pro-apoptotic pathway to direct the cells to undergo apoptotic cell death. The study throws light on the potential cytotoxicity of AFB_1 on humans and animals those are exposed to mycotoxin contaminated wheat grains.

ACKNOWLEDGEMENTS
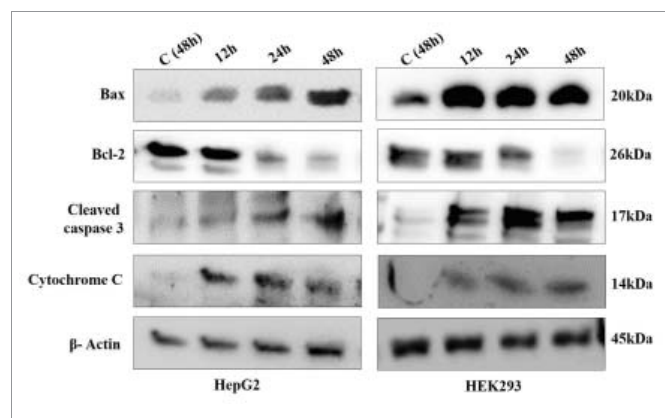
Figure 5: Western blot analysis of the expression of different pro-apoptotic and anti-apoptotic proteins in AFB_1 treated cells at different time intervals.
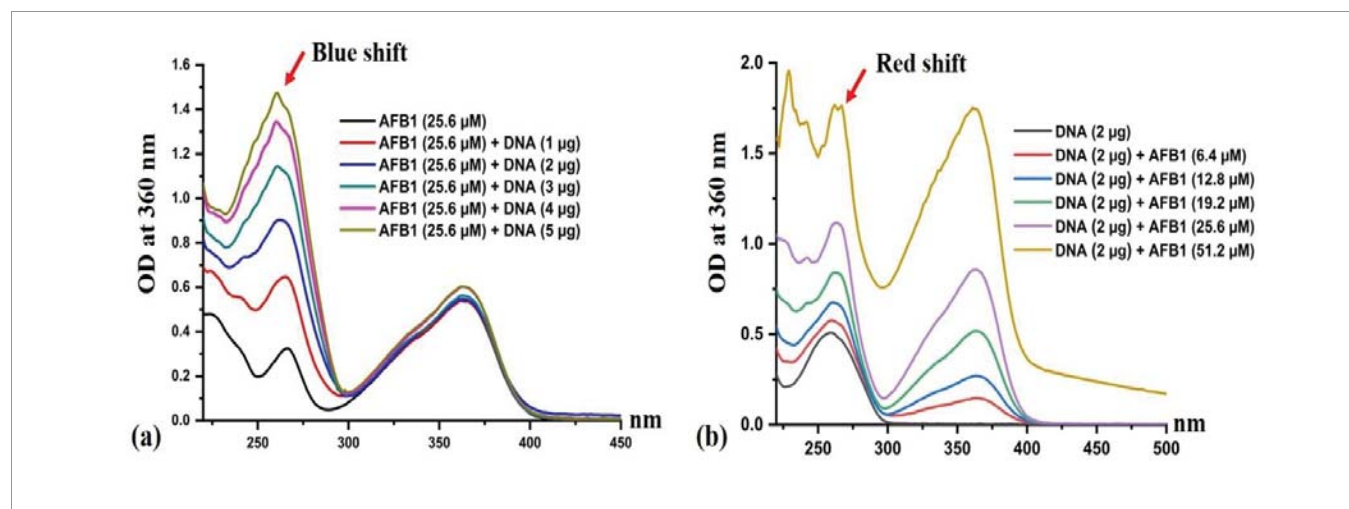
Figure 6: UV-visible absorption spectra of AFB_1-DNA complex (a) in the presence of fixed amount AFB1 with varying concentrations of fungal genomic DNA and (b) in the presence of fixed amount of fungal genomic DNA with varying concentrations of AFB_1.

REFERENCES

1. Alshannaq A, Yu JH. Occurrence, Toxicity, and Analysis of Major Mycotoxins in Food. Int J Environ Res Public Health. 2017 Jun 13;14(6):632. doi: 10.3390/ijerph14060632. PMID: 28608841; PMCID: PMC5486318.

2. Liu Y, Wu F. Global burden of aflatoxin-induced hepatocellular carcinoma: a risk assessment. Environ Health Perspect. 2010 Jun;118(6):818-824. doi: 10.1289/ehp.0901388. Epub 2010 Feb 19. PMID: 20172840; PMCID: PMC2898859.

3. Liu Y, Chang CC, Marsh GM, Wu F. Population attributable risk of aflatoxin-related liver cancer: systematic review and meta-analysis. Eur J Cancer. 2012 Sep;48(14):2125-2136. doi: 10.1016/j.ejca.2012.02.009. Epub 2012 Mar 8. PMID: 22405700; PMCID: PMC3374897.

4. Bedard LL, Alessi M, Davey S, Massey TE. Susceptibility to aflatoxin B1-induced carcinogenesis correlates with tissue-specific differences in DNA repair activity in mouse and in rat. Cancer Res. 2005 Feb 15;65(4):1265-70. doi: 10.1158/0008-5472.CAN-04-3373. PMID: 15735011.

5. Hamid AS, Tesfamariam IG, Zhang Y, Zhang ZG. Aflatoxin B1-induced hepatocellular carcinoma in developing countries: Geographical distribution, mechanism of action and prevention. Oncol Lett. 2013 Apr;5(4):1087-1092. doi: 10.3892/ol.2013.1169. Epub 2013 Jan 31. PMID: 23599745; PMCID: PMC3629261.

6. McKean C, Tang L, Tang M, Billam M, Wang Z, Theodorakis CW, Kendall RJ, Wang JS. Comparative acute and combinative toxicity of aflatoxin B1 and fumonisin B1 in animals and human cells. Food Chem Toxicol. 2006 Jun;44(6):868-876. doi: 10.1016/j.fct.2005.11.011. Epub 2006 Jan 19. PMID: 16427177.

7. Qureshi H, Hamid SS, Ali SS, Anwar J, Siddiqui AA, Khan NA. Cytotoxic effects of aflatoxin B1 on human brain microvascular endothelial cells of the blood-brain barrier. Med Mycol. 2015 May;53(4):409-416. doi: 10.1093/mmy/myv010. PMID: 25851265.

8. Sun LH, Lei MY, Zhang NY, Gao X, Li C, Krumm CS, Qi DS. Individual and combined cytotoxic effects of aflatoxin B1, zearalenone, deoxynivalenol and fumonisin B1 on BRL 3A rat liver cells. Toxicon. 2015 Mar;95:6-12. doi: 10.1016/j.toxicon.2014.12.010. Epub 2014 Dec 27. PMID: 25549941.

9. Mughal MJ, Xi P, Yi Z, Jing F. Aflatoxin B1 invokes apoptosis via death receptor pathway in hepatocytes. Oncotarget. 2017 Jan 31;8(5):8239-8249. doi: 10.18632/oncotarget.14158. PMID: 28030812; PMCID: PMC5352397.

10. Zhou H, George S, Hay C, Lee J, Qian H, Sun X. Individual and combined effects of Aflatoxin B$_1$, Deoxynivalenol and Zearalenone on HepG2 and RAW 264.7 cell lines. Food Chem Toxicol. 2017 May;103:18-27. doi: 10.1016/j.fct.2017.02.017. Epub 2017 Feb 20. PMID: 28223122.

11. Wu Q, Jezkova A, Yuan Z, Pavlikova L, Dohnal V, Kuca K. Biological degradation of aflatoxins. Drug Metab Rev. 2009;41(1):1-7. doi: 10.1080/03602530802563850. PMID: 19514968.

12. Kumari R, Jayachandran LE, Ghosh AK. Investigation of diversity and dominance of fungal biota in stored wheat grains from governmental warehouses in West Bengal, India. J Sci Food Agric. 2019 May;99(7):3490-3500. doi: 10.1002/jsfa.9568. Epub 2019 Feb 10. PMID: 30623426.

13. Plumb JA. Cell sensitivity assays: the MTT assay. Methods Mol Med. 2004;88:165-169. doi: 10.1385/1-59259-406-9:165. PMID: 14634227.

14. Kielkopf CL, Bauer W, Urbatsch IL. Bradford Assay for Determining Protein Concentration. Cold Spring Harb Protoc. 2020 Apr 1;2020(4):102269. doi: 10.1101/pdb.prot102269. PMID: 32238597.

15. Green M R, Hughes H, Sambrook J, MacCallum P. Molecular cloning: a laboratory manual. Cold Spring Harbor Laboratory Press, New York .2012;pp:1890-1890.

16. Ma L, Wang J, Zhang Y. Probing the Characterization of the Interaction of Aflatoxins B1 and G1 with Calf Thymus DNA In Vitro. Toxins (Basel). 2017 Jul 1;9(7):209. doi: 10.3390/toxins9070209. PMID: 28671585; PMCID: PMC5535156.

17. Lei M, Zhang N, Qi D. In vitro investigation of individual and combined cytotoxic effects of aflatoxin B1 and other selected mycotoxins on the cell line porcine kidney 15. Exp Toxicol Pathol. 2013 Nov;65(7-8):1149-1157. doi: 10.1016/j.etp.2013.05.007. Epub 2013 Jul 1. PMID: 23809186.

18. Golli-Bennour EE, Kouidhi B, Bouslimi A, Abid-Essefi S, Hassen W, Bacha H. Cytotoxicity and genotoxicity induced by aflatoxin B1, ochratoxin A, and their combination in cultured Vero cells. J Biochem Mol Toxicol. 2010 Jan-Feb;24(1):42-50. doi: 10.1002/jbt.20310. PMID: 20175139.

19. Rasooly R, Hernlem B, He X, Friedman M. Non-linear relationships between aflatoxin B□ levels and the biological response of monkey kidney vero cells. Toxins (Basel). 2013 Aug 14;5(8):1447-1461. doi: 10.3390/toxins5081447. PMID: 23949006; PMCID: PMC3760045.

20. Cummings BS, Schnellmann RG. Measurement of cell death in mammalian cells. Curr Protoc Pharmacol. 2004 Sep 1;Chapter 12:Unit 12.8. doi: 10.1002/0471141755.ph1208s25. PMID: 22294120; PMCID: PMC3874588.

21. Webster KA. Mitochondrial membrane permeabilization and cell death during myocardial infarction: roles of calcium and reactive oxygen species. Future Cardiol. 2012 Nov;8(6):863-884. doi: 10.2217/fca.12.58. PMID: 23176689; PMCID: PMC3562717.

22. Kamp HG, Eisenbrand G, Schlatter J, Würth K, Janzowski C. Ochratoxin A: induction of (oxidative) DNA damage, cytotoxicity and apoptosis in mammalian cell lines and primary cells. Toxicology. 2005 Jan 31;206(3):413-425. doi: 10.1016/j.tox.2004.08.004. PMID: 15588931.

23. Liu K, Liu PC, Liu R, Wu X. Dual AO/EB staining to detect apoptosis in osteosarcoma cells compared with flow cytometry. Med Sci Monit Basic Res. 2015 Feb 9;21:15-20. doi: 10.12659/MSMBR.893327. PMID: 25664686; PMCID: PMC4332266.

24. Xu B, Chu F, Zhang Y, Wang X, Li Q, Liu W, Xu X, Xing Y, Chen J, Wang P, Lei H. A Series of New Ligustrazine-Triterpenes Derivatives as Anti-Tumor Agents: Design, Synthesis, and Biological Evaluation. Int J Mol Sci. 2015 Sep 2;16(9):21035-21055. doi: 10.3390/ijms160921035. PMID: 26404253; PMCID: PMC4613240.

25. Rieger AM, Nelson KL, Konowalchuk JD, Barreda DR. Modified annexin V/propidium iodide apoptosis assay for accurate assessment of cell death. J Vis Exp. 2011 Apr 24;(50):2597. doi: 10.3791/2597. PMID: 21540825; PMCID: PMC3169266.

26. Sur E, Celik I. Effects of aflatoxin B1 on the development of the bursa of Fabricius and blood lymphocyte acid phosphatase of the chicken. Br Poult Sci. 2003 Sep;44(4):558-566. doi: 10.1080/00071660310001618352. PMID: 14584846.

27. Chen K, Shu G, Peng X, Fang J, Cui H, Chen J, Wang F, Chen Z, Zuo Z, Deng J, Geng Y, Lai W. Protective role of sodium selenite on histopathological lesions, decreased T-cell subsets and increased apoptosis of thymus in broilers intoxicated with aflatoxin B□. Food Chem Toxicol. 2013 Sep;59:446-454. doi: 10.1016/j.fct.2013.06.032. Epub 2013 Jun 28. PMID: 23810797.

28. Yang C, Fan J, Zhuang Z, Fang Y, Zhang Y, Wang S. The role of NAD(+)-dependent isocitrate dehydrogenase 3 subunit α in AFB1 induced liver lesion. Toxicol Lett. 2014 Jan 30;224(3):371-379. doi: 10.1016/j.toxlet.2013.10.037. Epub 2013 Nov 5. PMID: 24211421.

29. Peng X, Yu Z, Liang N, Chi X, Li X, Jiang M, Fang J, Cui H, Lai W, Zhou Y, Zhou S. The mitochondrial and death receptor pathways involved in the thymocytes apoptosis induced by aflatoxin B1. Oncotarget. 2016 Mar 15;7(11):12222-12234. doi: 10.18632/oncotarget.7731. PMID: 26933817; PMCID: PMC4914280.

30. Yin H, Jiang M, Peng X, Cui H, Zhou Y, He M, Zuo Z, Ouyang P, Fan J, Fang J. The molecular mechanism of G2M cell cycle arrest induced by AFB1 in the jejunum. Oncotarget. 2016 Jun 14;7(24):35592-35606. doi: 10.18632/oncotarget.9594. PMID: 27232757; PMCID: PMC5094947.

31. Li H, Li S, Yang H, Wang Y, Wang J, Zheng N. l-Proline Alleviates Kidney Injury Caused by AFB1 and AFM1 through Regulating Excessive Apoptosis of Kidney Cells. Toxins (Basel). 2019 Apr 16;11(4):226. doi: 10.3390/

toxins11040226. PMID: 30995739; PMCID: PMC6521284.

32. Liu Y, Du M, Zhang G. Proapoptotic activity of aflatoxin B$_1$ and sterigmatocystin in HepG2 cells. Toxicol Rep. 2014 Oct 29;1:1076-1086. doi: 10.1016/j.toxrep.2014.10.016. PMID: 28962319; PMCID: PMC5598229.

33. Kannan K, Jain S K. Oxidative stress and apoptosis. Pathophysiology. 2000;7:153-163.

34. Ozben T. Oxidative stress and apoptosis: impact on cancer therapy. J Pharm Sci. 2007 Sep;96(9):2181-2196. doi: 10.1002/jps.20874. PMID: 17593552.

35. George BP, Abrahamse H. Increased Oxidative Stress Induced by *Rubus* Bioactive Compounds Induce Apoptotic Cell Death in Human Breast Cancer Cells. Oxid Med Cell Longev. 2019 Jun 3;2019:6797921. doi: 10.1155/2019/6797921. PMID: 31281587; PMCID: PMC6589211.

36. Chen J, Chen K, Yuan S, Peng X, Fang J, Wang F, Cui H, Chen Z, Yuan J, Geng Y. Effects of aflatoxin B1 on oxidative stress markers and apoptosis of spleens in broilers. Toxicol Ind Health. 2016 Feb;32(2):278-284. doi: 10.1177/0748233713500819. Epub 2013 Oct 4. PMID: 24097364.

37. Aramesh-Boroujeni Z, Khorasani-Motlagh M, Noroozifar M. Multispectroscopic DNA-binding studies of a terbium(III) complex containing 2,2'-bipyridine ligand. J Biomol Struct Dyn. 2016;34(2):414-426. doi: 10.1080/07391102.2015.1038585. Epub 2015 Jun 23. PMID: 25994049.